

# Steady state velocity distribution of driven granular gases

V. V. Prasad,<sup>1,2,3</sup> Dibyendu Das,<sup>4</sup> Sanjib Sabhapandit,<sup>5</sup> and R. Rajesh<sup>2,3</sup>

<sup>1</sup>*Department of Physics of Complex Systems, Weizmann Institute of Science, Rehovot 7610001, Israel*

<sup>2</sup>*The Institute of Mathematical Sciences, C.I.T. Campus, Taramani, Chennai-600113, India*

<sup>3</sup>*Homi Bhabha National Institute, Training School Complex, Anushakti Nagar, Mumbai-400094, India*

<sup>4</sup>*Department of Physics, Indian Institute of Technology, Bombay, Powai, Mumbai-400076, India*

<sup>5</sup>*Raman Research Institute, Bangalore - 560080, India*

(Dated: June 12, 2025)

A central result of the kinetic theory of driven, inelastic gases is that the tail of the velocity distribution is a stretched exponential function with an exponent  $3/2$ . However, a derivation of this result starting from a microscopic model is lacking. We consider a microscopic model for a driven inelastic gas where a noise is added during each dissipative collision with a wall. We show by exact analysis that, for physically relevant noise distributions, the tail of the velocity distribution is a Gaussian with additional logarithmic corrections, in contradiction to the kinetic theory result.

PACS numbers: 81.05.Rm,47.45.-n,47.45.Ab,51.10.+y,05.40.-a

The velocity distribution of a gas in equilibrium is well-known to be Maxwellian (Gaussian). What is the velocity distribution for a collection of inelastic particles that is driven to a steady state through continuous injection of energy? This is the central question in the kinetic theory for dilute inelastic gases — which is widely used in developing phenomenological models for driven granular systems. Within kinetic theory, which ignores correlations between pre-collision velocities (molecular chaos hypothesis), for homogeneous driving, the tail of the velocity distribution is a stretched exponential  $P(v) \sim \exp(-a|v|^\beta)$  with a universal exponent  $\beta = 3/2$  [1]. This result is counterintuitive as it implies that larger speeds are more probable in inelastic systems than the corresponding elastic system with the same mean energy. A derivation of the kinetic theory result starting from a microscopic model is lacking, also experiments and large scale simulations (see below) are unable to unambiguously determine the tails of the distribution and hence, a convincing answer to the question is still lacking. In this paper, starting from a microscopic model for a driven inelastic gas, using exact analysis we show that, for physically relevant noise distributions,  $\beta = 2$ , albeit with additional logarithmic corrections such that the tails of the velocity distribution fall off slightly faster than Gaussian.

The tails of the velocity distribution have been studied in several experiments and large scale computer simulations. Experimental systems of driven granular gases comprise of collections granular particles such as steel balls or glass beads that undergo inelastic collisions and is driven either through collisions with vibrating walls [2–12] or by application of volume forces using electric [14, 15] or magnetic fields [16]. Some of the experiments observe a universal stretched exponential form with  $\beta \approx 1.5$  for various parameters of the system [2, 7, 9, 14], while other experiments find that  $\beta$  is dependent on the driving parameters and is non-universal and varies between 1 and 2 [6, 8, 10]. Numerical simula-

tions [17–19] have also been inconclusive. For a granular gas in three dimensions, driven homogeneously with a momentum conserving noise, it was shown that  $\beta \approx 1.5$  for large inelasticity, while  $\beta$  approaches 2 for more elastic systems [17]. Similar study on a bounded two dimensional granular system find  $\beta \approx 2$  for a range of coefficient of restitution and density [18, 19] while molecular dynamics simulations of a uniformly heated granular gas with solid friction find  $\beta = 2$  [20]. The determination of the tails of distributions in experiments and simulations suffer from poor sampling of tails as well as the presence of strong crossovers from the behaviour of the distribution at small velocities to the asymptotic behaviour at high velocities, making analysis difficult.

Theoretical approaches have either used kinetic theory, or studied simple analytically tractable models which capture the essential physics. Within kinetic theory [21], the non-linear Boltzmann equation, describing the time evolution of the single particle velocity distribution function in the presence of a diffusion term describing driving, is analysed. The asymptotic behaviour of the velocity distribution, obtained by linearizing the Boltzmann equation and balancing the diffusive term with the collisional loss term, is characterized by  $\beta = (2 + \delta)/2$  [1], where  $\delta$  describes the dependence of rate of collisions on the relative velocity  $\Delta v$  as  $|\Delta v|^\delta$ . For ballistic motion, since  $\delta = 1$ , one obtains  $\beta = 3/2$ . The study of simple models have been mostly restricted to inelastic Maxwell gases [22, 23] where each pair of particles collide at the same rate ( $\delta = 0$ ). The driving is of two kinds: diffusive driving (random acceleration) where a Gaussian white noise is added to the velocity of a particle, or dissipative driving where a particle colliding inelastically with a wall loses energy while receiving a kick. For diffusive driving and Gaussian noise, the velocity distribution for a one-component Maxwell gas has a universal exponential tail ( $\beta = 1$ ) independent of the coefficient of restitution [24–26], consistent with  $\delta = 0$  in the kinetic theory result.

However, the noise need not always be Gaussian. For a one-component Maxwell gas with arbitrary noise statistics and dissipative driving, it has been shown that the velocity distribution tails are non-universal and asymptotically follow same statistics as the noise [27]. This result continues to hold for arbitrary  $\delta > 0$  [28].

Diffusive driving has the drawback that it causes the velocity of the centre of mass to diffuse. This leads to a continuous heating up of the system, and correlations amongst the velocities grow with time [1]. Thus, such systems do not reach a steady state. However, the results that have been derived for diffusive driving has been interpreted to describe a system whose reference frame is attached to the center of mass [1, 30]. Therefore, a priori, it is not clear whether such theory or numerical simulations describe experimental situations where measurements are performed in the laboratory reference frame and the external driving is not momentum conserving. Dissipative driving, on the other hand, drives the system to a steady state [1] and is closer to an experimental situation. In this paper, we consider a microscopic model for a two-component granular gas with dissipative driving, which as a special case includes diffusive driving also. By analysing the equation satisfied by large moments, we obtain that  $\beta = 2$  with additional logarithmic corrections, provided the noise distribution decays faster than a Gaussian, i.e,

$$\ln P(\mathbf{v}) = -a|\mathbf{v}|^2(\ln|\mathbf{v}|)^\tau + \dots, \tau > 0, |\mathbf{v}|^2 \gg \langle |\mathbf{v}|^2 \rangle. \quad (1)$$

For elastic wall collisions, we obtain  $\beta = [2 + \min(\delta, 0)]/2$ . If the noise distribution decays slower than gaussian (exponential for elastic wall collisions), then the velocity distribution is non-universal and has the same statistics as the noise distribution. We argue that realistic noise distributions fall off faster than a Gaussian, and hence  $P(\mathbf{v})$  is generically as described in Eq. (1), in contradiction to the results from kinetic theory. A discussion is developed as to elucidate the reason behind the kinetic theory failing to capture this result.

Consider a system of  $N$  identical particles labelled by  $i = 1, \dots, N$ , having two dimensional velocities  $\mathbf{v}_i$ . Particles  $i$  and  $j$  undergo momentum conserving inelastic collision at a rate  $\frac{2\lambda_c}{N-1}|\mathbf{v}_i - \mathbf{v}_j|^\delta$ , and the new velocities  $\mathbf{v}'_i$  and  $\mathbf{v}'_j$  are given by

$$\begin{aligned} \mathbf{v}'_i &= \mathbf{v}_i - \alpha [(\mathbf{v}_i - \mathbf{v}_j) \cdot \hat{\boldsymbol{\sigma}}] \hat{\boldsymbol{\sigma}}, \\ \mathbf{v}'_j &= \mathbf{v}_j + \alpha [(\mathbf{v}_i - \mathbf{v}_j) \cdot \hat{\boldsymbol{\sigma}}] \hat{\boldsymbol{\sigma}}, \end{aligned} \quad (2)$$

where  $\alpha = (1+r)/2$ ,  $r$  being the coefficient of restitution, and  $\hat{\boldsymbol{\sigma}}$  is a unit vector along the line joining the centres of the particles at contact. We will assume that  $\hat{\boldsymbol{\sigma}}$  is randomly oriented. Note that we have a well-mixed system, as is done in kinetic theory, such that spatial information is ignored. Since  $r \in [0, 1)$ , we obtain  $\alpha \in [1/2, 1)$ . A particle  $i$  undergoes a collision with a wall at rate  $\lambda_d$

and the new velocity  $\mathbf{v}'_i$  is given by [1]

$$\mathbf{v}'_i = -r_w \mathbf{v}_i + \boldsymbol{\eta}, \quad (3)$$

where  $r_w$  is the coefficient of restitution for particle-wall collisions and the noise  $\boldsymbol{\eta}$  is uncorrelated in time, and drawn from a fixed distribution. Note that diffusive driving may be realized by setting  $r_w = -1$  in Eq. (3). Equation (3) may be derived by assuming that the wall is massive compared to the particles and that the collision times are random [1]. We characterize the isotropic noise distribution  $\Phi(\boldsymbol{\eta})$  by its asymptotic behaviour

$$\Phi(\eta_{x,y}) \sim e^{-b|\eta_{x,y}|^\gamma}, \quad b, \gamma > 0, \quad |\eta_{x,y}| \gg \sigma_\eta, \quad (4)$$

where  $\sigma_\eta^2$  is the second moment. It is not necessary that  $\boldsymbol{\eta}$  is a Gaussian with  $\gamma = 2$ . For example, for a sinusoidally oscillating wall, if the collision times are assumed to be random, then it is straightforward to show that  $\Phi(\boldsymbol{\eta}) \sim (c^2 - \eta^2)^{-1/2}$ , with  $\eta \in (-c, c)$ , corresponding to  $\gamma = \infty$ .

For the sake of clarity, we present results for the case  $\delta = 0$ , when the rate of collision becomes independent of the relative velocity, corresponding to the Maxwell gas. For this special case, the equations are less unwieldy. The extension to non-zero  $\delta$  is straightforward and outlined at the end of the paper.

We first show that the system reaches a steady state when  $r_w \neq -1$ . The equations obeyed by the set of two-point correlation functions close and may be solved explicitly (see Supplemental Information for details). In the steady state, we find the second moments to be

$$\begin{aligned} \langle v_{x,y}^2 \rangle &= \frac{2\lambda_d \sigma_\eta^2}{\lambda_c(1-r^2) + 2\lambda_d(1-r_w^2)} \\ &+ \frac{1}{N} \frac{\lambda_c^2 \sigma_\eta^2 (1-r^2)^2}{2(1+r_w)[\lambda_c(1-r^2) + 2\lambda_d(1-r_w^2)]^2} + \mathcal{O}(N^{-2}). \end{aligned} \quad (5)$$

The two particle correlations for both  $x$  and  $y$  components is  $\mathcal{O}(1/N)$  and vanish in the thermodynamic limit, while the  $xy$  correlations are identically zero due to symmetry. For diffusive driving ( $r_w = -1$ ), the second moment diverges as may be seen from the  $\mathcal{O}(N^{-1})$  term in Eq. (5), showing the absence of a steady state. For collision kernels with  $\delta \neq 0$ , the equations for the two-point correlation functions do not close among themselves, however it may be shown numerically that the system reaches a steady state similar to the case  $\delta = 0$  (see Supplemental Information for details).

The tails of the velocity distribution may be inferred by knowing the large moments of the velocity. Let  $M_{2n} = \langle v_x^{2n} \rangle$ . From Eqs. (2) and (3) we obtain:

$$M_{2n} = \frac{\lambda_c}{K} \sum_{m=1}^{n-1} t_m + \frac{\lambda_d}{K} \sum_{m=0}^{n-1} \binom{2n}{2m} r_w^{2m} M_{2m} \mathcal{N}_{2n-2m}, \quad (6)$$

where  $K = \lambda_c + \lambda_d(1-r_w^2)$ ,  $\mathcal{N}_{2m} = \langle \eta_x^{2m} \rangle$ , and

$$t_m = \int_0^{2\pi} \frac{d\theta}{2\pi} \binom{2n}{2m} \langle (a_1 v_x + a_2 v_y)^{2n-2m} \rangle \langle (a_3 v_x + a_4 v_y)^{2m} \rangle, \quad (7)$$

where  $a_1 = 1 - \alpha \cos^2 \theta$ ,  $a_2 = -\alpha \cos \theta \sin \theta$ ,  $a_3 = 1 - a_1$ , and  $a_4 = -a_2$ . The first sum in the right hand side of Eq. (6) has its origin in inter-particles collisions while the second sum arises from driving. Since the driving is isotropic, the velocity distribution is also isotropic and hence is a function of only the modulus of velocity. Thus, we write

$$P(\mathbf{v}) \sim e^{-a|\mathbf{v}|^\beta + \Psi(|\mathbf{v}|)}, \quad a, \beta > 0, |\mathbf{v}|^2 \gg \langle v^2 \rangle, \quad (8)$$

where the correction term is such that  $|\mathbf{v}|^{-\beta} \Psi(|\mathbf{v}|) \rightarrow 0$ . The large moments  $M_{2n} \equiv \langle v_x^{2n} \rangle = \langle v_y^{2n} \rangle$  for this distribution may be determined using a saddle point approximation (see Supplemental Information for more details):

$$M_{2n} \sim \left[ \frac{2n}{a\epsilon\beta} \right]^{\frac{2n}{\beta}} n^{\frac{2-\beta}{\beta}} e^{\Psi[(\frac{2n}{a\beta})^{\frac{1}{\beta}}]}, \quad n \gg 1, \quad (9)$$

$$\langle (a_i v_x + a_j v_y)^{2n} \rangle \sim M_{2n} (a_i + a_j)^n. \quad (10)$$

The odd moments vanish due to symmetry.

It is clear that the moments in Eq. (9), and hence the terms in Eq. (6), diverge exponentially with  $n$ . Therefore, the sums in the right hand side of Eq. (6) may be approximated by the largest terms with negligible error. We solve Eq. (6) keeping in the right hand side only the first (second) sum, and denote the corresponding solution for  $\beta$  by  $\beta_c$  ( $\beta_d$ ), where the subscripts  $c$  and  $d$  denote collision and driving respectively. Clearly,

$$\beta = \min(\beta_c, \beta_d). \quad (11)$$

The calculation of the exponent  $\beta_d$  is identical to that for the one component granular gas, where it may be shown exactly that [27, 28]:

$$\beta_d = \begin{cases} \gamma, & r_w < 1, \\ \min \left[ \frac{2+\min(\delta, 0)}{2}, \gamma \right], & r_w = 1, \end{cases} \quad (12)$$

where additional logarithmic corrections are present when  $r_w = 1, \delta > 0$ . For the one component gas  $\beta_c = \infty$ , and thus  $\beta = \beta_d$  [28]. However, for the two component gas, it turns out that  $\beta_c \neq \infty$ , as we show below.

To obtain  $\beta_c$ , we look for self-consistent solutions for Eq. (6) when the second sum in the right hand side is dropped. For large  $n$ , the summation  $\sum_m t_m$  may be converted to an integral by changing variables to  $y = m/n$ . We evaluate the integrals over  $\theta$  and  $y$  by the saddle point approximations, valid for large  $n$  (see Supplemental Information for more details). For  $\beta_c > 2$ , the maximum occurs for  $0 < y^* < 1$ . We then obtain for  $\beta_c > 2$ :

$$M_{2n} \sim \frac{n^{\frac{4}{\beta_c}}}{n^{5/2}} \left[ \frac{2n}{a\epsilon\beta_c} \right]^{\frac{2n}{\beta_c}} \left[ \frac{1}{1-y^*} \right]^{\frac{n(\beta_c-2)}{\beta_c}} \times e^{\Psi[(\frac{2n(1-y^*)}{a\beta_c})^{\frac{1}{\beta_c}}] + \Psi[(\frac{2ny^*}{a\beta_c})^{\frac{1}{\beta_c}}]}, \quad (13)$$

$$y^* = \frac{\alpha^{\frac{\beta_c}{\beta_c-2}}}{\alpha^{\frac{\beta_c}{\beta_c-2}} + (2-\alpha)^{\frac{\beta_c}{\beta_c-2}}}. \quad (14)$$

The result for  $M_{2n}$  in Eq. (13) is not consistent with the expression in Eq. (9) due to the extra exponential term in Eq. (13). The only way to compensate for this term is if the subleading correction  $\Psi(x) \sim x^{\beta_c}$ . However, this contradicts our assumption that  $\Psi(x)x^{-\beta_c} \rightarrow 0$ . Thus, we conclude that our assumption of  $\beta_c > 2$  must be incorrect and hence, we obtain the bound:

$$\beta_c \leq 2. \quad (15)$$

For  $\beta_c \leq 2$ , the maximal contribution from the integral comes from the endpoint  $\alpha_1 = 0$ . Then, the scaling  $m = yn$  breaks down and it is possible that the maximal contribution to the first sum in Eq. (6) comes from a term with  $m^* \sim n^\phi$  with  $\phi < 1$ , where  $t_{m^*} \approx t_{m^*+1}$ . To determine  $m^*$ , we first evaluate  $t_m$  [see Eq. (7)] in the limit  $m \ll n$  to obtain

$$t_m \approx \frac{(2n\alpha)^{2m}}{(2m)!} n^{\frac{2-\beta_c}{\beta_c}} \left( \frac{2n}{a\epsilon\beta_c} \right)^{\frac{2n}{\beta_c}} \left( \frac{2n}{a\beta_c} \right)^{\frac{-2m}{\beta_c}} e^{\Psi[(\frac{2n}{a\beta})^{\frac{1}{\beta}}]} \times \sum_{j=0}^m \frac{\langle v_x^{2j} v_y^{2m-2j} \rangle \Gamma(j+m+1/2)}{[\alpha(2-\alpha)n]^{m+j+1/2}}. \quad (16)$$

For large  $n$ , the sum in the right hand side of Eq. (16) is dominated by the term  $j = 0$ , as every successive term is smaller by a factor of  $n$ . Taking the ratio of successive terms, we obtain

$$\frac{t_{m+1}}{t_m} \approx \frac{\alpha}{(2-\alpha)} \left( \frac{a\beta_c}{2} \right)^{\frac{2}{\beta_c}} \frac{\langle v_y^{2m+2} \rangle}{m \langle v_y^{2m} \rangle} \frac{1}{n^{\frac{2-\beta_c}{2}}}, \quad \frac{m}{n} \rightarrow 0. \quad (17)$$

When  $\beta_c < 2$ , each successive term  $t_m$  is smaller by a factor  $n^{\frac{2-\beta_c}{2}}$ . Thus, the largest term is  $t_1$ , and therefore, from Eq. (16), we obtain

$$M_{2n} \sim t_1 \sim n^{\frac{2-\beta_c}{\beta_c} + (\frac{1}{2} - \frac{2}{\beta_c})} \left( \frac{2n}{a\epsilon\beta_c} \right)^{\frac{2n}{\beta_c}} e^{\Psi[(\frac{2n}{a\beta})^{\frac{1}{\beta}}]} \quad (18)$$

Comparing with the expression for  $M_{2n}$  in Eq. (9), we obtain  $1/2 - 2/\beta_c = 0$  or  $\beta_c = 4$  which contradicts our assumption that  $\beta_c < 2$ . Thus,  $\beta_c \geq 2$ . This result, together with Eq. (15) imply that

$$\beta_c = 2. \quad (19)$$

We now check when  $\beta_c = 2$  is a self-consistent solution.

When  $\beta_c = 2$  the ratio of successive terms  $t_m$ , as in Eq. (17), simplifies to

$$\frac{t_{m+1}}{t_m} \approx \frac{\alpha a}{(2-\alpha)} \frac{\langle v_y^{2m+2} \rangle}{m \langle v_y^{2m} \rangle}, \quad \frac{m}{n} \rightarrow 0, \quad \beta_c = 2. \quad (20)$$

When  $m \sim n^\phi$  with  $0 < \phi < 1$ , then the moments of the velocity may be evaluated using Eq. (9) to obtain  $\langle v_y^{2m+2} \rangle / (m \langle v_y^{2m} \rangle) = a^{-1}$ , such that  $t_{m+1}/t_m = \alpha/(2-\alpha) < 1$ . This implies that successive terms are smaller,

and therefore the solution for  $m^*$  is such that  $m^* \sim n^0$ . For any such  $m^*$ , it is straightforward to obtain from Eq. (16) that  $M_{2n} \sim t_{m^*} \sim M_{2n}/\sqrt{n}$  which is not a consistent solution.

We note that for  $\beta_c > 2$ , the collision sum overestimates  $M_{2n}$  [see Eq. (13)] while it underestimates  $M_{2n}$  for  $\beta_c \leq 2$ . To obtain additional power law factors of  $\mathcal{O}(\sqrt{n})$  for  $\beta_c = 2$ , we require  $\langle v_y^{2m} \rangle$  in Eq. (17) to depend on  $n$ , such that  $m^* \sim n^\phi$  with  $\phi > 0$ . This is possible if there are additional logarithmic corrections present in the velocity distribution such that

$$P(\mathbf{v}) \sim \exp[-a|\mathbf{v}|^2(\ln|\mathbf{v}|)^\tau], \quad a, |\mathbf{v}|^2 \gg \langle v^2 \rangle. \quad (21)$$

For such a distribution, it may be shown that

$$\frac{t_{m+1}}{t_m} \approx \frac{\alpha}{2-\alpha} \left[ \frac{\ln n}{\ln m} \right]^\tau \quad m \ll n. \quad (22)$$

Setting the ratio to 1, we obtain  $m^* \sim n^\phi$ , where  $\phi = [\alpha/(2-\alpha)]^{1/\tau}$ . Since  $\phi < 1$ , we require  $\tau > 0$ , such that the distribution decays faster than a gaussian. Determining  $\tau$  requires keeping more than the first few terms in the asymptotic behaviour of moments.

The exponent  $\beta$  is now determined from Eqs. (11), (12) and (19). Generically, collisions with the wall are inelastic ( $r_w < 1$ ). Also, noise distributions typically have a largest velocity, corresponding to large  $\gamma$ . Thus we conclude that the tails of the velocity distribution are generically a gaussian with additional logarithmic corrections, as described in Eq. (1).

The extension to non-zero  $\delta$  is straightforward. For this case, it is clear that the velocity dependent collision rate adds a power law correction of the form  $n^{\delta/\beta}$  to the different moments. However, in the calculation of  $\beta_c$ , the entire argument was based on the terms that were exponential in  $n$ , and these arguments still go through for the case  $\delta \neq 0$ , without altering the value of  $\beta_c$ . An example of an explicit calculation with non-zero  $\delta$  may be found in Ref. [28] for the one-component system. We note that non-zero  $\delta$  affects the result for  $\beta_d$  for elastic collisions with the wall [see Eq. (12)].

The results from Monte Carlo simulations with isotropic driving are consistent with the results for  $\beta$  that we have obtained (see Supplemental Information). Here, we present results for the steady state velocity distribution when driving is restricted to the  $x$ -component, mimicking many experiments [5–10, 12] where particles are driven in one direction and the distribution of the component perpendicular to the driving is measured. Figure 1 shows the results for the distribution when the noise distribution  $\Phi(\eta)$  is uniform ( $\gamma = \infty$ ) in  $[-3/2, 3/2]$  (main panel) and an exponential ( $\gamma = 1$ ) (inset). In the former case, the  $P(v_y)$  is consistent with a Gaussian, while in the latter, it is consistent with an exponential distribution, as predicted by our calculation.

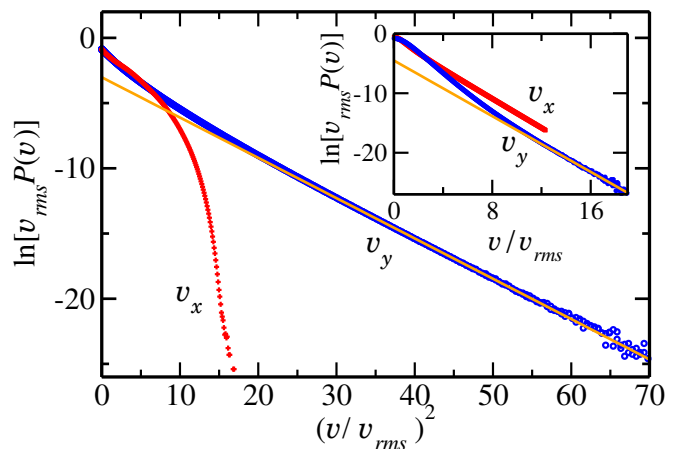


FIG. 1. (Color Online) The steady states velocity distribution ( $x$ , and  $y$  components) of a two-component Maxwell gas when only the  $x$ -component is driven, as obtained from Monte Carlo simulations. The data are for when the noise distribution  $\Phi(\eta)$  is uniform in  $[-3/2, 3/2]$  (main panel), and an exponential (inset). The solid straight lines are guides to the eye.

We note that the experimental data for the measurement of  $P(v)$  may be open to interpretation. As an example, by re-plotting, we show that the data obtained in a recent experiment [2] with homogeneous driving is consistent with  $\beta = 2$  [see Supplemental Material].

We now discuss why kinetic theory result ( $\beta = 3/2$ ) differs from ours ( $\beta = 2$  with logarithmic corrections). In kinetic theory, the steady state one particle scaled velocity distribution  $P(v)$  satisfies [1]:

$$-c_1 v^\delta P(v) + c_2 \frac{\partial^2}{\partial v^2} P(v) = 0, \quad (23)$$

where the two terms describe collisional losses and driving. Assuming  $P(v) \sim \exp(-av^\beta)$ , it is easy to show that Eq. (23) implies  $\beta = (2 + \delta)/2$ ; for  $\delta = 1$  (in the ballistic case),  $\beta = 3/2$  [1]. The diffusive driving term in Eq. (23) may be derived from our model when  $r_w = 1$  and Taylor-expanding for small  $\eta$ . However, it may be shown that truncation at  $\mathcal{O}(\eta^2)$  is not valid for  $\delta > 0$  when considering the tails of the distribution, and that the largest term in the Taylor expansion corresponding to a higher order derivative. Boltzmann equation with a dissipative term,

$$-c_1 v^\delta P(v) + c_2 \frac{\partial^2}{\partial v^2} P(v) + \Gamma \frac{\partial}{\partial v} [vP(v)] = 0, \quad (24)$$

has also been studied where the origin of the dissipation is due to either near-elastic wall collisions [31] or thermostating [32, 33]. By balancing the second and third terms and ignoring inter-particle collisions, one obtains  $\beta = 2$ . However, neither does it capture the logarithmic corrections, nor does it capture the correct physics, as the origin of  $\beta = 2$  in our calculation is inter-particle collisions.

This research was supported in part by the International Centre for Theoretical Sciences (ICTS) during a visit for participating in the program -Indian Statistical Physics Community Meeting 2016 (Code: ICTS/Prog-ISPC/2016/02)

- 
- [1] T. van Noije and M. Ernst, *Granular Matter* **1**, 57 (1998).
- [2] E. Clement and J. Rajchenbach, *Europhys. Lett.* **16**, 133 (1991).
- [3] S. Warr, J. M. Huntley, and G. T. H. Jacques, *Phys. Rev. E* **52**, 5583 (1995).
- [4] A. Kudrolli, M. Wolpert, and J. P. Gollub, *Phys. Rev. Lett.* **78**, 1383 (1997).
- [5] J. S. Olafsen and J. S. Urbach, *Phys. Rev. Lett.* **81**, 4369 (1998).
- [6] J. S. Olafsen and J. S. Urbach, *Phys. Rev. E* **60**, R2468 (1999).
- [7] W. Losert, D. G. W. Cooper, J. Delour, A. Kudrolli, and J. P. Gollub, *Chaos* **9**, 682 (1999).
- [8] A. Kudrolli and J. Henry, *Phys. Rev. E* **62**, R1489 (2000).
- [9] F. Rouyer and N. Menon, *Phys. Rev. Lett.* **85**, 3676 (2000).
- [10] D. L. Blair and A. Kudrolli, *Phys. Rev. E* **64**, 050301 (2001).
- [11] G. Baxter and J. Olafsen, *Nature* **425**, 680 (2003).
- [12] J. S. van Zon, J. Kreft, D. I. Goldman, D. Miracle, J. B. Swift, and H. L. Swinney, *Phys. Rev. E* **70**, 040301 (2004).
- [2] C. Scholz and T. Pöschel, *Phys. Rev. Lett.* **118**, 198003 (2017).
- [14] I. S. Aranson and J. S. Olafsen, *Phys. Rev. E* **66**, 061302 (2002).
- [15] K. Kohlstedt, A. Snezhko, M. V. Sapozhnikov, I. S. Aranson, J. S. Olafsen, and E. Ben-Naim, *Phys. Rev. Lett.* **95**, 068001 (2005).
- [16] M. Schmick and M. Markus, *Phys. Rev. E* **78**, 010302 (2008).
- [17] S. J. Moon, M. D. Shattuck, and J. B. Swift, *Phys. Rev. E* **64**, 031303 (2001).
- [18] J. S. van Zon and F. C. MacKintosh, *Phys. Rev. Lett.* **93**, 038001 (2004).
- [19] J. S. van Zon and F. C. MacKintosh, *Phys. Rev. E* **72**, 051301 (2005).
- [20] P. Das, S. Puri, and M. Schwartz, *Granular Matter* **20**, 15 (2018).
- [21] N. Brilliantov and T. Pöschel, *Kinetic theory of granular gases* (Oxford University Press, USA, 2004).
- [22] A. V. Bobylev, J. A. Carrillo, and I. M. Gamba, *J. Stat. Phys.* **98**, 743 (2000).
- [23] E. Ben-Naim and P. L. Krapivsky, *Phys. Rev. E* **61**, R5 (2000).
- [24] M. H. Ernst and R. Brito, *Phys. Rev. E* **65**, 040301 (2002).
- [25] T. Antal, M. Droz, and A. Lipowski, *Phys. Rev. E* **66**, 062301 (2002).
- [26] A. Santos and M. H. Ernst, *Phys. Rev. E* **68**, 011305 (2003).
- [27] V. V. Prasad, D. Das, S. Sabhapandit, and R. Rajesh, *Phys. Rev. E* **95**, 032909 (2017).
- [28] V. V. Prasad and R. Rajesh, arXiv preprint arXiv:1803.11031 (2018).
- [1] V. V. Prasad, S. Sabhapandit, and A. Dhar, *Europhys. Lett.* **104**, 54003 (2013).
- [30] D. R. M. Williams and F. C. MacKintosh, *Phys. Rev. E* **54**, R9 (1996).
- [31] V. V. Prasad, S. Sabhapandit, and A. Dhar, *Phys. Rev. E* **90**, 062130 (2014).
- [32] M. J. Montanero and A. Santos, *Granular Matter* **2**, 53 (2000).
- [33] T. Biben, P. Martin, and J. Piasecki, *Physica A* **310**, 308 (2002).

## Supplemental material for Steady state velocity distribution of driven granular gases

### EXACT EVALUATION OF THE TWO-POINT CORRELATION FUNCTION

In this section, we calculate the steady state two point correlations of the two-component Maxwell gas ( $\delta = 0$ ). We follow closely the method of calculation used for determining the same for the one-component Maxwell gas [S1]. The system evolves through inter-particle collisions [see Eq. (2) in main text] at a rate  $\frac{2\lambda_c}{N-1}$  and each particle is driven [Eq. (3) in main text] at rate  $\frac{\lambda_d}{N-1}$ .

We are interested in the evolution of the two-point correlation functions

$$\begin{aligned}\Sigma_0^x(t) &= \frac{1}{N} \sum_i \langle v_{ix}(t)v_{ix}(t) \rangle, & \Sigma_{12}^x(t) &= \frac{1}{N(N-1)} \sum_{i \neq j} \langle v_{ix}(t)v_{jx}(t) \rangle, \\ \Sigma_0^y(t) &= \frac{1}{N} \sum_i \langle v_{iy}(t)v_{iy}(t) \rangle, & \Sigma_{12}^y(t) &= \frac{1}{N(N-1)} \sum_{i \neq j} \langle v_{iy}(t)v_{jy}(t) \rangle, \\ \Sigma_0^{xy}(t) &= \frac{1}{N} \sum_i \langle v_{ix}(t)v_{iy}(t) \rangle, & \Sigma_{12}^{xy}(t) &= \frac{1}{N(N-1)} \sum_{i \neq j} \langle v_{ix}(t)v_{jy}(t) \rangle.\end{aligned}\tag{S1}$$

From the dynamics, it is possible to obtain the exact evolution of the two-point functions as a set of coupled equations, which may be written in a compact form

$$\frac{d\mathbf{\Sigma}(t)}{dt} = \mathbf{R}\mathbf{\Sigma}(t) + \mathbf{C}.\tag{S2}$$

Here, the column vectors,  $\mathbf{\Sigma}^T$ ,  $\mathbf{C}^T$  are given by:

$$\begin{aligned}\mathbf{\Sigma}(t) &= [\Sigma_0^x(t), \Sigma_{12}^x(t), \Sigma_0^y(t), \Sigma_{12}^y(t), \Sigma_0^{xy}(t), \Sigma_{12}^{xy}(t)]^T, \\ \mathbf{C} &= [\sigma^2/N, 0, \sigma^2/N, 0, 0, 0]^T,\end{aligned}$$

and  $\mathbf{R}$  is the matrix

$$\begin{bmatrix} -[A_1 + A_2(1 - r_w)] & \frac{A_1}{N-1} & \frac{A_3}{(N-1)} & -\frac{A_3}{(N-1)} & 0 & 0 \\ \frac{A_1}{N-1} & \frac{-[A_1 + 2A_2(N-1)]}{N-1} & \frac{-A_3}{(N-1)} & \frac{A_3}{(N-1)} & 0 & 0 \\ A_3 & -A_3 & -[A_1 + A_2(1 - r_w)] & A_1 & 0 & 0 \\ \frac{-A_3}{N-1} & \frac{A_3}{N-1} & \frac{A_1}{(N-1)} & \frac{-[A_1 + 2A_2(N-1)]}{(N-1)} & 0 & 0 \\ 0 & 0 & 0 & 0 & -(A_4 + A_2) & A_4 \\ 0 & 0 & 0 & 0 & \frac{A_4}{N-1} & \frac{-A_4 + A_2(N-1)}{N-1} \end{bmatrix}.\tag{S3}$$

The constants  $\{A_i\}$ 's are function of the rates  $\lambda_c$ ,  $\lambda_d$  as well as the coefficient of restitutions,  $\alpha = (1+r)/2$  and  $r_w$ :

$$\begin{aligned}A_1 &= \lambda_c(2\alpha - 3\alpha^2/2), & A_2 &= \lambda_d(1 + r_w), \\ A_3 &= \lambda_c\alpha^2/2, & A_4 &= \lambda_c(2\alpha - \alpha^2).\end{aligned}$$

In the steady state the left hand side of Eq. (S2) may be equated to zero. Solving the resulting linear equation, we obtain the steady state values of the different correlation functions as

$$\Sigma_0^x = \Sigma_0^y = \frac{\lambda_d\sigma^2}{2\alpha(1-\alpha)\lambda_c + (1-r_w^2)\lambda_d} + \frac{2\alpha^2(1-\alpha)^2\lambda_c^2\sigma^2}{(1+r_w)[2\alpha(1-\alpha)\lambda_c + (1-r_w^2)\lambda_d]^2} \frac{1}{N} + O(N^{-2}),\tag{S4}$$

and

$$\Sigma_{12}^x = \Sigma_{12}^y = \frac{2\alpha(1-\alpha)\lambda_c^2\sigma^2}{(1+r_w)[2\alpha(1-\alpha)\lambda_c + (1-r_w^2)\lambda_d]^2} \frac{1}{N} + O(N^{-2}).\tag{S5}$$

When  $r_w \neq -1$ , the limit  $N \rightarrow \infty$  is well defined with finite value for  $\Sigma_0$  [Eq. (S4)] but the correlations  $\Sigma_{12}$  [Eq. (S5)] vanishes as  $O(1/N)$ . However, when  $r_w = -1$ ,  $\Sigma_0^{x,y} = \infty$  implying the absence of steady state. Note that, this is not the case when  $r_w = 1$  for which  $\Sigma_0^{x,y}$  has a finite value.

In Fig. S1 and Fig. S2, the time evolution of  $\Sigma_0$ , as obtained from Monte Carlo simulations, is shown for the cases  $\delta = 0$  and  $\delta = 1$  respectively. For diffusive driving ( $r_w = -1$ ), shown in the left panel of Fig. S1 we find that for large

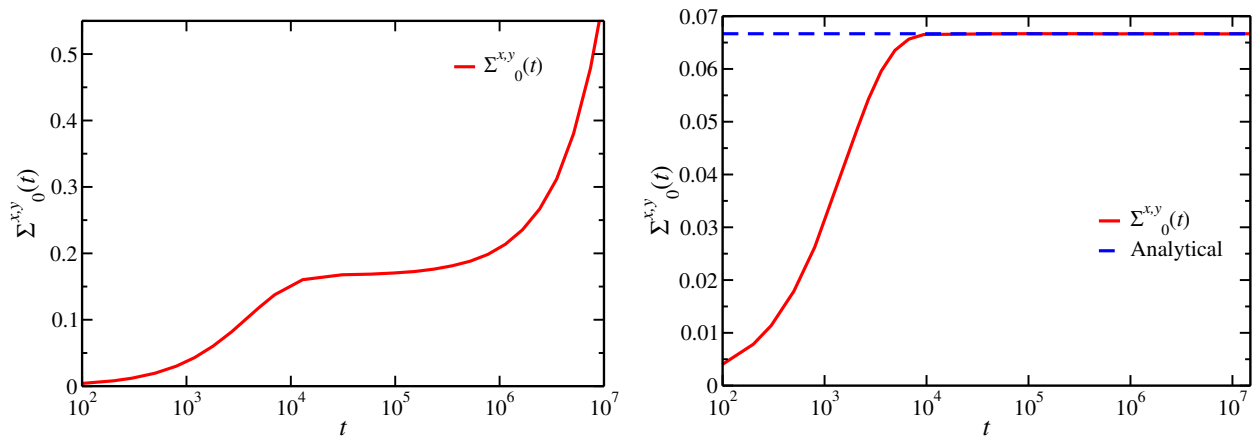


FIG. S1. The time evolution of the variance  $\Sigma_0^{x,y}(t)$  for a Maxwell gas ( $\delta = 0$ ) of  $N = 1000$  particles and  $r = 0$ . Note that the x-axis is logarithmic. The left panel shows the evolution when the driving is diffusive ( $r_w = -1$ ). The monotonic increase in the variance in the large time limit illustrates the lack of steady state for the system. The right panel show the data for dissipative driving with  $r_w = 1/2$ . The system reaches a stationary state. The dotted lines denotes the analytically obtained steady state value. In both the cases, the noise  $\eta$  is drawn from a uniform distribution with  $\sigma^2 = 1/12$  and  $\lambda_c = \lambda_d = 1/2$ .

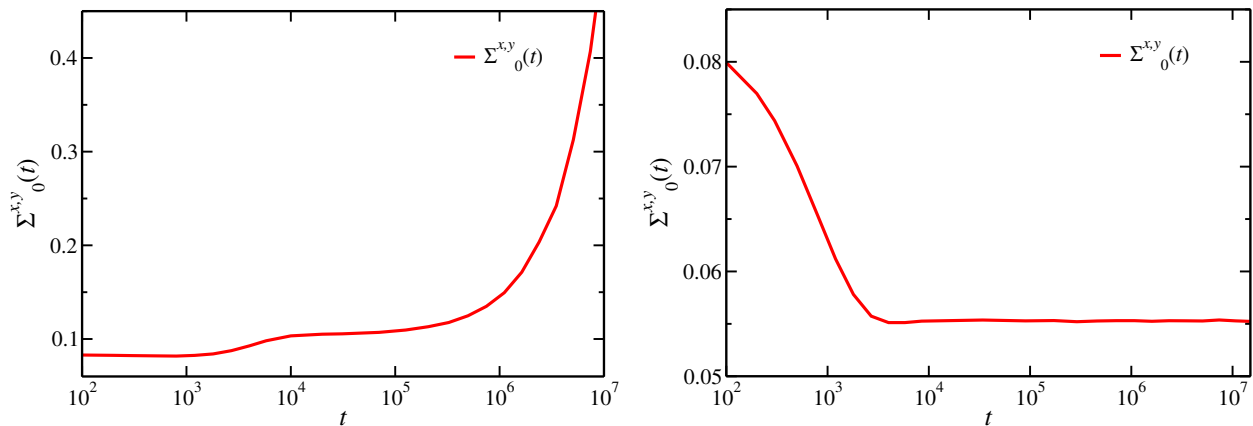


FIG. S2. The time evolution of the variance  $\Sigma_0^{x,y}(t)$  for a granular gas ( $\delta = 1$ ). Note that the x-axis is logarithmic. The left panel shows the evolution when the driving is diffusive ( $r_w = -1$ ). The monotonic increase in the variance in the large time limit illustrates the lack of steady state for the system. The right panel show the data for dissipative driving with  $r_w = 1/2$ . The system reaches a stationary state. In both the cases, the noise  $\eta$  is drawn from a uniform distribution with  $\sigma^2 = 1/12$  and  $\lambda_c = \lambda_d = 1/2$ .

times the variance  $\Sigma_0$  does not saturate but increases monotonically as a function of time, showing that the system does not have a steady state as shown by the analytical calculation. The lack of steady state is caused by the diffusion of the centre of mass due to the additive noise in the driving that do not conserve the total momentum. For  $r_w \neq 1$  the system reaches a steady state, as seen in the right panel of Fig. S1 which shows the time evolution of  $\Sigma_0$  for the case  $r_w = 1/2$ . The numerically obtained steady state value coincides with the analytically obtained value.

The analytical calculation cannot be extended to a general collision kernel where the collision rate can depend on the relative velocities ( $\delta \neq 0$ ). It is, however, possible to perform a Monte Carlo simulation for such systems. The Fig. S2 shows the time evolution of the mean energy of a system with  $\delta = 1$  (ballistic gas). The results are qualitatively the same as that obtained for the case  $\delta = 0$ . For diffusive driving ( $r_w = -1$ ) the system does not reach a steady state (left panel of Fig. S2). However, for  $r_w \neq -1$  the system reaches a steady state as seen in the right panel of Fig. S2.

## LARGE MOMENTS–ASYMPTOTIC BEHAVIOUR

In the following, we derive the asymptotic form for the moments of the velocity distribution for large  $n$ . Consider an isotropic velocity distribution having the form:

$$P(\mathbf{v}) \sim e^{-a|\mathbf{v}|^\beta + \Psi(|\mathbf{v}|)}, \quad a, \beta > 0, |\mathbf{v}|^2 \gg \langle v^2 \rangle, \quad (\text{S6})$$

and  $\Psi(|\mathbf{v}|)/|\mathbf{v}|^\beta \rightarrow 0$ . We would like to compute the moments of  $(a_i v_x + a_j v_y)^{2n}$ , for large  $n$ . This may be formally written as

$$\langle (a_i v_x + a_j v_y)^{2n} \rangle \sim \int dv_x dv_y (a_i v_x + a_j v_y)^{2n} e^{a(v_x^2 + v_y^2)^{\frac{\beta}{2}} + \Psi((v_x^2 + v_y^2)^{\frac{1}{2}})} \quad (\text{S7})$$

Changing variables to  $v_x = n^{1/\beta} t$  and  $v_y = n^{1/\beta} u$  the integral in Eq. (S7) may be rewritten as

$$\langle (a_i v_x + a_j v_y)^{2n} \rangle \sim n^{\frac{2}{\beta}} n^{\frac{2n}{\beta}} \int dt du e^{nf(u,t)} e^{\Psi\left(n^{\frac{1}{\beta}} [t^2 + u^2]^{\frac{1}{2}}\right)}, \quad (\text{S8})$$

where

$$f(u, t) = 2 \ln[a_i t + a_j u] - b(t^2 + u^2)^{\frac{\beta}{2}}. \quad (\text{S9})$$

Doing a saddle point integration by maximising  $f(u, t)$  with respect to the variables  $u$  and  $t$ , we obtain:

$$\langle (a_i v_x + a_j v_y)^{2n} \rangle \sim n^{\frac{2+2n}{\beta}} e^{\Psi\left(n^{\frac{1}{\beta}} [t^{*2} + u^{*2}]^{\frac{1}{2}}\right)} \frac{e^{nf(t^*, u^*)}}{n}, \quad n \gg 1, \quad (\text{S10})$$

where the integration over  $u$  and  $t$  pulls down a factor  $1/n$ .  $(t^*, u^*)$  is the point at which  $f$  has a maximum,

$$t^* = \frac{a_i}{\sqrt{a_i^2 + a_j^2}} \frac{2}{a\beta}, \quad (\text{S11})$$

$$u^* = \frac{a_j}{\sqrt{a_i^2 + a_j^2}} \frac{2}{a\beta}. \quad (\text{S12})$$

Substituting for  $t^*$  and  $u^*$  in Eq. (S10), we obtain

$$\langle (a_i v_x + a_j v_y)^{2n} \rangle \sim \left(\frac{2n}{ae\beta}\right)^{\frac{2n}{\beta}} n^{\frac{2}{\beta}-1} e^{\Psi\left(\left[\frac{2n}{a\beta}\right]^{\frac{1}{\beta}}\right)} (a_i^2 + a_j^2)^n, \quad n \gg 1, \quad (\text{S13})$$

and in particular, when  $a_i = 1$  and  $a_j = 0$ , the result simplifies to

$$M_{2n} = \langle v_x^{2n} \rangle \sim \left(\frac{2n}{ae\beta}\right)^{\frac{2n}{\beta}} n^{\frac{2}{\beta}-1} e^{\Psi\left(\left[\frac{2n}{a\beta}\right]^{\frac{1}{\beta}}\right)}, \quad n \gg 1. \quad (\text{S14})$$

## COLLISION SUM: ASYMPTOTIC EXPRESSION

In this section we consider the collision contribution in the moment equation [Eq. (6) in main text],

$$I = \sum_{m=1}^{n-1} \binom{2n}{2m} \int_0^{2\pi} \frac{d\theta}{2\pi} \langle (a_1 v_x + a_2 v_y)^{2n-2m} \rangle \langle (a_3 v_x + a_4 v_y)^{2m} \rangle \quad (\text{S15})$$

with

$$\begin{aligned} a_1 &= 1 - \alpha \cos^2 \theta, & a_2 &= -\alpha \cos \theta \sin \theta \\ a_3 &= 1 - a_1, & \text{and} & \quad a_4 = -a_2. \end{aligned} \quad (\text{S16})$$

Using the asymptotic expression for the moments [Eq. (S13)], it may be seen that each of the terms in the sum grown exponentially with  $n$  and therefore we perform the sum by the saddle point approximation. Taking Stirling's approximation, substituting the values of  $a_i$ 's and converting the sum to integral with respect to a variable  $y = m/n$  Eq. (S15) becomes,

$$I \sim n^{\frac{4}{\beta} - \frac{3}{2}} \int_0^1 dy \int_0^{2\pi} \frac{d\theta}{2\pi} [y(1-y)]^{\frac{2}{\beta} - \frac{3}{2}} e^{\Psi\left(\left[\frac{2n(1-y)}{a\beta}\right]^{\frac{1}{\beta}}\right)} e^{\Psi\left(\left[\frac{2n(y)}{a\beta}\right]^{\frac{1}{\beta}}\right)} e^{nf(\theta,y)}, \quad (\text{S17})$$

with

$$f(\theta, y) = \frac{2(1-\beta)}{\beta} [y \ln y + (1-y) \ln(1-y)] - (1-y) \ln[1 - \alpha(2-\alpha) \cos^2 \theta] + y \ln(\alpha^2 \cos^2 \theta) \quad (\text{S18})$$

The function  $f(\theta, y)$  is maximised when  $\theta = \theta_{1,2}^*$  and  $y = y^*$ . It is easily obtained that

$$\theta_1^* = 0, \quad \pi, \quad (\text{S19})$$

$$\cos^2(\theta_2^*) = \frac{y_2^*}{\alpha[1-\alpha]}. \quad (\text{S20})$$

For  $\theta = \theta_1^*$  we obtain

$$y_1^* = \alpha^{\frac{\beta}{\beta-1}} \left[ \alpha^{\frac{\beta}{\beta-1}} + (1-\alpha)^{\frac{\beta}{\beta-1}} \right]^{-1}, \quad (\text{S21})$$

$$f(\theta_1^*, y_1^*) = \frac{2(\beta-1)}{\beta} \ln \left[ \alpha^{\frac{\beta}{\beta-1}} + (1-\alpha)^{\frac{\beta}{\beta-1}} \right], \quad (\text{S22})$$

and for  $\theta = \theta_2^*$ ,

$$y_2^* = \alpha^{\frac{\beta}{\beta-2}} \left[ \alpha^{\frac{\beta}{\beta-2}} + (2-\alpha)^{\frac{\beta}{\beta-2}} \right]^{-1}, \quad \cos^2 \theta_2^* = \frac{y_1^*}{\alpha(1-\alpha)}, \quad (\text{S23})$$

$$f(\theta_2^*, y_2^*) = \frac{(\beta-2)}{\beta} \ln \left[ \frac{\alpha^{\frac{\beta}{\beta-2}} + (2-\alpha)^{\frac{\beta}{\beta-2}}}{(2-\alpha)^{\frac{\beta}{\beta-2}}} \right]. \quad (\text{S24})$$

A straightforward analysis of the two solutions may be performed to check which has a larger value for  $f$ . Specifically, when  $\beta > 2$  the  $f(\theta, y)$  has a maximum at  $(\theta_2^*, y_2^*)$ , but when  $\beta \leq 2$  it is at  $(0,0)$ .

## MONTE-CARLO RESULTS FOR THE VELOCITY DISTRIBUTION WITH ISOTROPIC DRIVING

We perform Monte-Carlo simulation to obtain the steady state distribution for the 2D-Maxwell gas ( $\delta = 0$ ) driven by wall collision [Eq. (2) in main text]. In Fig. S3, we show the variation of the scaled distribution of the absolute velocity,  $v_{rms}P(|\mathbf{v}|)$  with speed, for isotropic driving. The main panel shows the probability distribution when the noise distribution  $\Phi(\boldsymbol{\eta})$  is a uniform distribution in the range  $|\boldsymbol{\eta}| < 1$  corresponding to  $\gamma = \infty$ . When plotted against  $(|\mathbf{v}|/v_{rms})^2$ , the linear behaviour for large velocities is consistent with our prediction of  $\beta_c = 2$  for  $\gamma > 2$  [see Eq. (19) in main text]. The inset shows the velocity distribution, when the noise distribution  $\Phi(\boldsymbol{\eta})$  is an exponential, corresponding to  $\gamma = 1$ . When plotted against  $(|\mathbf{v}|/v_{rms})$ , the linear behaviour for large velocities is consistent with our prediction of  $\beta = \gamma$  for  $\gamma \leq 2$ .

## ANALYSIS OF THE EXPERIMENTAL RESULT

In this section, we compare the data from for the velocity distribution from recent experiments [S2] on a driven granular gas in two dimensions with our results. The experiment involved a system of particles residing on a two-dimensional surface which is driven through a periodic motion of the surface so that the steady state of the system is homogeneous. We extract the data for the velocity distribution from Fig. 5 of Ref. [S2] and plot the data both as a function of the  $(v/v_{rms})^{3/2}$  and as a function of  $(v/v_{rms})^2$ . Clearly, the data cannot be used to distinguish between the two distributions. If anything, the Gaussian describes the data better.

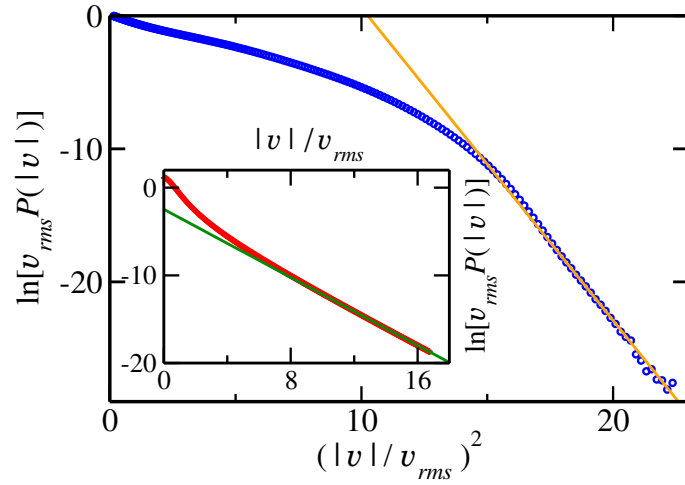


FIG. S3. Results from Monte Carlo simulations for the scaled distribution  $v_{rms}P(|\mathbf{v}|)$  for a 2D Maxwell gas ( $\delta = 0$ ) for isotropic driving [see Eqs. (4) and (5) in main text]. The main plot shows the scaled distribution plotted against  $(|\mathbf{v}|/v_{rms})^2$ , when the noise distribution  $|\boldsymbol{\eta}|$  is a uniform distribution, corresponding to  $\gamma = \infty$ . In the inset the data is for when the noise distribution  $|\boldsymbol{\eta}|$  is exponential. The scaled distribution is plotted against  $(|\mathbf{v}|/v_{rms})$ . The data are for  $r_w = 1/2$ ,  $r = 0$  and  $\lambda_c = \lambda_d = 1/2$ .

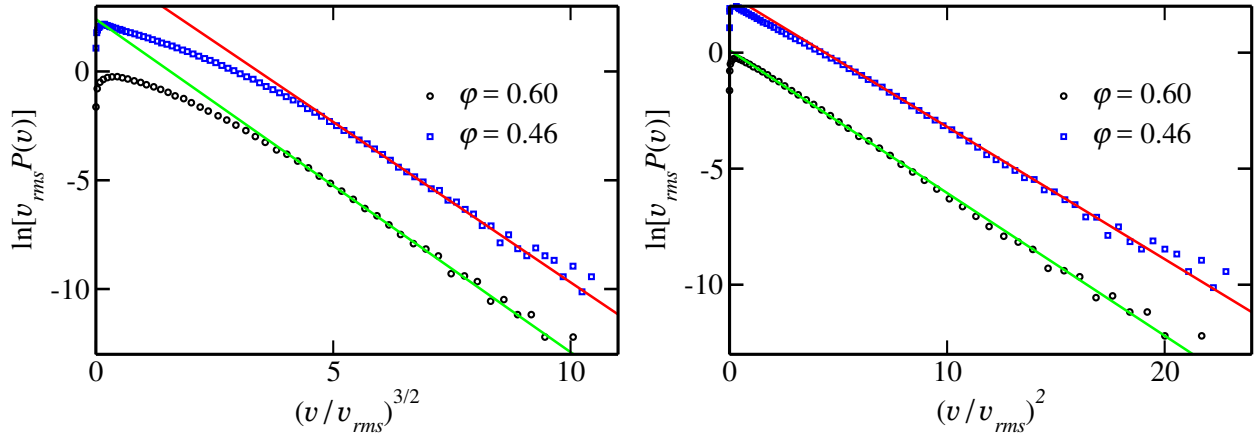


FIG. S4. Experimental data for the velocity distribution, extracted from Fig. 5 of Ref. [S2], is plotted as a function of  $(v/v_{rms})^{3/2}$  (left panel) and  $(v/v_{rms})^2$  (right panel). The data are for two different volume fractions  $\varphi$ . As in Ref. [S2] one of the data-set is shifted vertically for clarity. Solid straight lines are guides for the eye.

[S1] V. V. Prasad, S. Sabhapandit, and A. Dhar, *Europhys. Lett.* **104**, 54003 (2013).

[S2] C. Scholz and T. Pöschel, *Phys. Rev. Lett.* **118**, 198003 (2017).